Electronic Structure of the Transition-Metal Nitrates $Ti(NO_3)_4$, $VO(NO_3)_3$, $Co(NO_3)_3$, and $Cu(NO_3)_2$. Studied by Low-Energy Photoelectron Spectroscopy and ab Initio Molecular Orbital and Scattered Wave–Xα Calculations

C. D. Garner,*[1a] Roger W. Hawksworth,[1a] Ian H. Hillier,[1a] Alistair A. MacDowell,[1a] and Martyn F. Guest[1b]

Contribution from the Chemistry Department, Manchester University, Manchester M13 9PL, United Kingdom, and the Science Research Council Laboratory, Daresbury, Warrington, WA4 4AD, United Kingdom. *Received September 10, 1979*

Abstract: Low-energy (<22 eV) photoelectron spectra have been recorded for the transition-metal nitrates $Ti(NO_3)_4$, $VO(NO_3)_3$, $Co(NO_3)_3$, and $Cu(NO_3)_2$ in the gas phase. The interpretation of these spectra has been achieved with reference to ab initio molecular orbital and scattered wave Xα calculations. There are three regions in the spectra of all four molecules that clearly correlate with the ($1a_2'$, $1e''$, $4e'$), ($1a_2''$, $3e'$), and $4a_1'$ orbitals of the nitrate ion; the features in these three regions have been assigned, using Koopmans' theorem, to ionizations from the group molecular orbitals expected for the particular assembly of nitrato ligands. In the spectra of $Ti(NO_3)_4$, $Co(NO_3)_3$, and $Cu(NO_3)_2$, there are additional ionizations higher in energy than the first ligand band; these are assigned to ionization from metal–ligand bonding orbitals and are taken to indicate that strong metal–ligand bonding is achieved using the $4e'$ (oxygen $2p_\sigma$) orbitals of the nitrato groups. The assignment of the metal ionizations of $Co(NO_3)_3$ and $Cu(NO_3)_2$ has not been completely resolved. However, it is clear from the experimental data that in each case the lowest energy feature arises from metal ionizations. The ligand regions of the spectra also provide some information about the relative charge distributions in these four molecules. The ionization energy of the peak that correlates with the ($1a_2''$, $3e'$) nitrate orbitals is essentially the same for the Ti, V, and Co complexes but is some 0.3 eV smaller for the Cu complex. This difference is reflected in the formal charges calculated from the ab initio wave functions for the ligand (−0.53 e for $Ti(NO_3)_4$; −0.46 e for $Co(NO_3)_3$; −0.69 e for $Cu(NO_3)_2$) and which presumably arises from the greater number of d orbitals into which L → M electron donation can occur for Ti^{IV}, V^{V}, and Co^{III}, as compared to the Cu^{II} complex.

The simple, covalent, anhydrous metal nitrates are well characterized and typically exhibit remarkable reactivities.[2] However, little experimental or theoretical[3] work has been reported that gives direct information about the electronic structure of these molecules. Low-energy photoelectron (PE) spectroscopy should provide direct information on the ordering and energy of the filled molecular orbitals (MOs) of such molecules and therefore we have recorded the He(I) and He(II) PE spectra of $Ti(NO_3)_4$, $VO(NO_3)_3$, $Co(NO_3)_3$, and $Cu(NO_3)_2$. The two theoretical methods most widely used to calculate molecular ionization energies (IEs) are the ab initio SCF-MO and the scattered wave (SW)-Xα techniques. We have used both of these methods to describe the electronic structure and to calculate the IEs of $Co(NO_3)_3$ and $Cu(NO_3)_2$ which, together with the earlier ab initio calculation accomplished[3] for $Ti(NO_3)_4$, have aided the interpretation of the PE spectra obtained.

Experimental Section

$Ti(NO_3)_4$,[4,5] $VO(NO_3)_3$,[5] $Co(NO_3)_3$,[6] and $Cu(NO_3)_2$[7] were prepared and purified according to published procedures. He(I) and He(II) PE spectra of these gaseous molecules were obtained using the PE spectrometer described previously,[8] modified to allow gas-phase measurements to be made. The experimental conditions are summarized in Table I. The measured PE spectra are shown in Figures 1–4 and IEs are listed in Table II. The relative areas under certain bands are presented in Table III.

Interpretation of the Photoelectron Spectra

$Ti(NO_3)_4$[4] and $Co(NO_3)_3$[9] have been shown by X-ray crystallography to be comprised of discrete molecules containing four and three bidentate nitrato groups with molecular structures which closely correspond to D_{2d} and D_3 symmetry, respectively. Coordination leads to a polarization of the nitrate group which is clearly manifest in the relative length of the N–O bonds; those involving a coordinated oxygen atom (1.292 Å) are significantly longer than that (1.185 Å) involving the terminal oxygen. Although $Cu(NO_3)_2$ is polymeric in the solid state,[2] molecular-weight measurements[10] have established that the compound sublimes as the simple molecular species and electron-diffraction measurements have shown this to have D_{2d} symmetry with two bidentate nitrato groups. A gas-phase electron diffraction study[12] has shown that $VO(NO_3)_3$ also contains bidentate nitrato groups.

A molecular orbital (MO) description of the electronic structure of these $M(NO_3)_x$ molecules is expected to result in MOs that correlate with the valence orbitals of the nitrate ion, the symmetry correlations for which are presented in Table IV, together with orbitals of mainly metal 3d character. Thus, their PE spectra will have regions that resemble the PE spectrum of NO_3^-, perturbed by metal–nitrate bonding and the lowering of the symmetry from D_{3h}, plus, where appropriate, regions that have no counterpart in the spectrum of the ligand, corresponding to metal 3d ionizations.

The interpretation of the PE spectra of the nitrato complexes is thus aided by the availability of the PE spectra of the gaseous alkali metal nitrates.[13] The He(I) spectrum of KNO_3(g) is reproduced in Figure 1. The nitrate groups of this system may be taken as essentially ionic so that their PE spectrum can be interpreted in terms of the orbitals of NO_3^-. The ab initio calculations described earlier[8] for NO_3^- allow for a clear interpretation of the PE spectrum of KNO_3(g). The first band at ca. 10 eV, which has three components, arises due to ionizations from the $1a_2'$, $1e''$, and $4e'$ MOs of NO_3^- which are mainly oxygen 2p in character; the second band at ca. 16 eV, which has two components, is assigned to ionizations from the $3e'$ and $1a_2''$ MOs which are N–O bonding in character. Although no further ionizations are shown by the He(I) spectrum of KNO_3(g) the He(II) spectrum[8] of solid KNO_3 reveals a third band 2 eV to higher IE than the second band, which is assigned to ionizations from the $4a_1'$ MO.

$Ti(NO_3)_4$. The formal d^0 configuration of the metal atom in $Ti(NO_3)_4$ suggests that the PE spectrum of this molecule will be the simplest to interpret, with all the orbitals correlating with the nitrate orbitals as indicated in Table IV. Figure 1

0002-7863/80/1502-4325$01.00/0

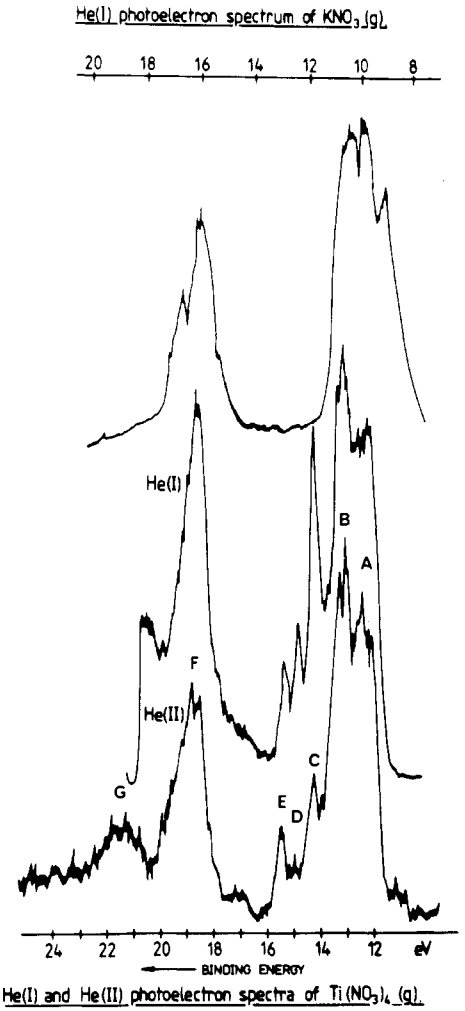

Figure 1. He(I) photoelectron spectrum of KNO_3(g) and He(I) and He(II) photoelectron spectrum of $Ti(NO_3)_4$(g).

Table I. Experimental Conditions for Observing Gas-Phase PE Spectra

compd	temp, °C	counts s^{-1} He(I)[a]	counts s^{-1} He(II)[b]
$Ti(NO_3)_4$	22	200	70
$VO(NO_3)_3$	22	1100	100
$Co(NO_3)_3$	22	550	550
$Cu(NO_3)_2$	148-158	220	220

[a] $\Delta\epsilon$ = 45-65 meV. [b] $\Delta\epsilon$ = 80-120 meV.

Table II. Ionization Energies[a] in Gas-Phase Spectra

region[b]	$Ti(NO_3)_4$	$VO(NO_3)_3$	$Co(NO_3)_3$	$Cu(NO_3)_2$
A	12.35(11)	12.33(4)	10.79(3)	10.47(4)
B	13.10(7)	13.03(6)	11.89(3)	11.65(4)
C	14.20(4)	13.65(3), 13.85(7)	12.42(11)	12.17(3)
D	14.85(4)	(17.48(6))[c]	12.85(15)	12.63(4), 13.06(5)
E	15.32(5)	18.83(6)[d]	13.28(4)	13.68(3)
F	18.80(10)[d]	21.10(10)[d]	14.66(4)	14.20(4)
G	21.34(15)[d]		15.57(7)	15.35(4)
H[d]			18.95(10)	18.50(15)
I[d]			21.85(15)	21.50(15)

[a] In eV with estimated probable error in parentheses. [b] See Figures 1-4. [c] Probably due to an impurity; see text. [d] He(II) spectral data.

Table III. Relative Peak[a] Intensities in He(II) Spectra

$Ti(NO_3)_4$	$Co(NO_3)_3$	$Cu(NO_3)_2$
	0.2 (A)	0.2 (A)
1.7 (A-E)	1.5 (B-G)	3.8 (B-G)
1.0 (F-G)	1.0 (H-I)	1.0 (H-I)

[a] See Figures 1, 3, and 4.

Table IV. Symmetry Correlations of Nitrate Valence Orbitals to Nitrato Complexes

NO_3^-	$Ti(NO_3)_4$	$VO(NO_3)_3$	$Co(NO_3)_3$	$Cu(NO_3)_2$
D_{3h}	D_{2d}	C_{3v}	D_3	D_{2d}
a_2'	a_1, b_2, e	a_1, e	a_2, e	e
e''	$2(a_2, b_1, e)$	$2(a_2, e)$	$a_1, a_2, 2e$	a_2, b_1, e
e'	$2(a_1, b_2, e)$	$2(a_1, e)$	$a_1, a_2, 2e$	a_1, b_2, e
a_2''	a_2, b_1, e	a_2, e	a_2, e	e
a_1'	a_1, b_2, e	a_1, e	a_1, e	a_1, b_2

Table V. Correlation between Ionization Energies (eV) of Valence Orbitals of NO_3^- and $Ti(NO_3)_4$

KNO_3 orbital	KNO_3 1E calcd[a]	KNO_3 1E exptl[b]	$Ti(NO_3)_4$ orbital	$Ti(NO_3)_4$ 1E calcd[c]	$Ti(NO_3)_4$ 1E exptl	assignment
			$3a_2$	14.9		
			18e	15.4		
$1a_2'$	9.9	9.0	$3b_1$	15.5		
			$15b_2$	16.0		
			17e	16.0	12.35(11)	(A)
$1e''$	9.9	9.9	16e	16.2		
			$16a_1$	16.4		
			$2a_2$	16.4		
			$2b_1$	16.6		
			$15a_1$	16.8		
			$14b_2$	16.9	13.10(7)	(B)
$4e'$	11.4	10.5	15e	17.0		
			14e	17.5	14.20(4)	(C)
			$13b_2$	18.7	14.85(4)	(D)
			$14a_1$	18.9	15.32(5)	(E)
			13e	22.7		
			$13a_1$	22.9		
$3e'$	17.5	16.1	$12b_2$	23.0		
			12e	23.5		
			$12a_1$	23.9	18.80(10)	(F)
			$1a_2$	24.2		
$1a_2''$	18.1	16.7	$11b_2$	24.3		
			11e	24.5		
			$1b_1$	24.8		
			10e	26.2		
$4a_1'$	20.7	18.8[a,d]	$10b_2$	26.4	21.34(15)	(G)
			$11a_1$	27.2		

[a] Reference 8. [b] KNO_3(g), ref 13. [c] Reference 3. [d] 0.7 eV lower than in KNO_3(g) by comparison with other 1E features of KNO_3(g).

shows that there is a close similarity between the PE spectrum[14] of $Ti(NO_3)_4$(g) and that of KNO_3(g); a shift in the energy scale for the former of some 3 eV to lower energy results in the two spectra being nearly superimposable, except that the spectrum of $Ti(NO_3)_4$(g) contains the additional peaks C, D, and E to high IE of the first broad band (A, B). The calculated orbital energies[3] for $Ti(NO_3)_4$ allow for a detailed interpretation of the PE spectrum of this molecule which is consistent with the general principles outlined thus far and Table V summarizes the correlation between the valence orbitals of NO_3^- and $Ti(NO_3)_4$. The lower energy region (A) of the first broad peak is assigned to a group of orbitals ($3a_2$-$2b_1$) which correlate with the $1a_2'$ and $1e''$ MOs of NO_3^-; the higher energy region (B) of the first broad peak is assigned to the $15a_1$,

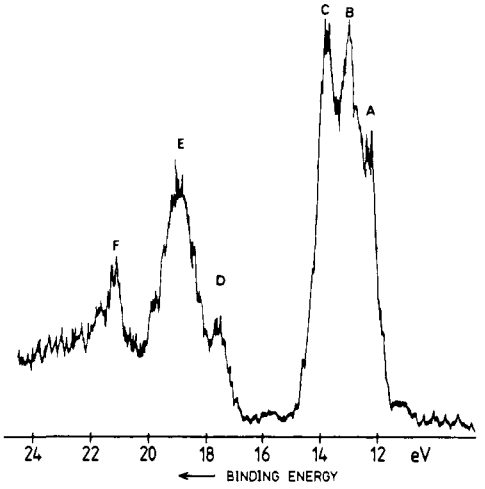

Figure 2. He(II) photoelectron spectrum of $VO(NO_3)_3(g)$.

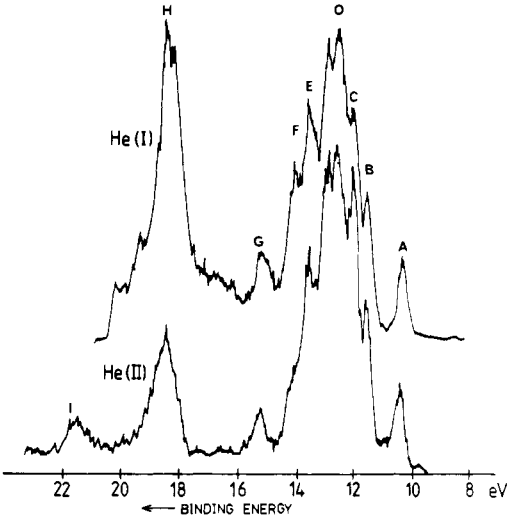

Figure 3. He(I) and He(II) photoelectron spectrum of $Cu(NO_3)_2(g)$.

$14b_2$, and 15e orbitals which correlate with the 4e′ MOs of the nitrato groups. The additional orbitals which correlate with these 4e′ MOs, the 14e, $13b_2$, and $14a_1$ MOs, are assigned to the higher energy peaks C, D, and E, respectively. These latter orbitals are calculated to have a small amount of metal character and to give rise to the metal–ligand bonding interactions, consistent with their displacement to higher IE from B. The profile of the He(I) PE spectrum of $Ti(NO_3)_4(g)$ (Figure 1) is similar to that of the He(II) spectrum for the region A, B, whereas peaks C, D, and E are relatively more intense in the He(I) spectrum. Although we attempt no detailed interpretation of the origin of these changes in relative intensity, they would appear to be a clear indication of a different atomic composition of the orbitals giving rise to the peaks C, D, and E, as compared to those associated with the region A, B. This is consistent with results of the ab initio calculation for this molecule[3] which attributed metal–ligand bonding characteristics to the former set of orbitals and the almost exclusive nitrate character to the latter. The broad band (F) in the $Ti(NO_3)_4(g)$ spectrum at 18.8 eV is assigned to ionizations from the group of orbitals ($13e-1b_1$) that correlate with the 3e′ and $1a_2''$ MOs of the nitrato groups. The highest IE feature in the He(II) spectrum (G) is assigned to the 10e, $10b_2$, and $11a_1$ MOs that correlate with the $4a_1'$ MOs of the nitrato groups. The shift of some 3 eV to higher IE observed for $Ti(NO_3)_4(g)$ as compared to $KNO_3(g)$ is probably associated with the smaller effective negative charge on the nitrato groups of the former as compared to the nitrate anion of the latter; the MO calculation[3] suggests that each nitrato group of $Ti(NO_3)_4(g)$ has a net charge of −0.53 e, whereas that for $KNO_3(g)$ is presumably ca. −1.0 e.

$VO(NO_3)_3$. The profile of the PE spectrum of the other formally d^0 system, $VO(NO_3)_3(g)$ (Figure 2), bears a closer overall resemblance to that of $KNO_3(g)$ than does that of $Ti(NO_3)_4(g)$. In the lowest energy region of the spectrum, the three peaks A, B, and C clearly correlate with the three components of the first band system of $KNO_3(g)$ and arise from MOs that correlate with the $1a_2'$, 1e″, and 4e′ MOs of the nitrato groups and, unlike $Ti(NO_3)_4(g)$, there are no features <2.5 eV above this first band system. These two observations suggest that the electronic structure of the nitrato groups is significantly less perturbed in $VO(NO_3)_3$ than in $Ti(NO_3)_4$ with the metal–nitrate covalent interactions being significantly weaker in the former molecule than in the latter. Peak D in the PE spectrum of $VO(NO_3)_3(g)$, which has no counterpart in the PE spectra of $Ti(NO_3)_4(g)$ or $KNO_3(g)$, could be assigned to ionizations from MOs of mainly oxygen 2p character and localized on the V–O group. However, as this occurs[15] at ca. 14 eV in $VOCl_3(g)$, it seems unlikely that this is correct. Thus we suggest that peak D is probably due to an unspecified impurity and note that a very weak feature is observed at a similar energy in $Ti(NO_3)_4$ (see Figure 1). The two highest IEs E and F in the PE spectrum of $VO(NO_3)_3(g)$ are attributed to ionizations from MOs that correlate with the 3e′ and $1a_2''$, and $4a_1'$ orbitals of the nitrato groups. Despite the comments above, IEs for the nitrate orbitals of $VO(NO_3)_3(g)$ are at a similar energy to those of $Ti(NO_3)_4(g)$, which suggests that the effective negative charge of the nitrato groups is similar in these two molecules.

$Cu(NO_3)_2$. The PE spectra recorded[14] for $Cu(NO_3)_2(g)$ are shown in Figure 3. The interpretation of this spectrum is complicated by the presence of ionizations from the mainly metal MOs which give rise to the formal d^9 configuration of the metal. The IEs of $Cu(NO_3)_2$ calculated by both ab initio and SW–Xα procedures are given later but it is possible to interpret the PE spectra with reference to the assignment presented for $Ti(NO_3)_4$. Peak A (Figure 3), which has no counterpart in the spectra of $Ti(NO_3)_4(g)$, must arise from metal ionizations which are absent in $Ti(NO_3)_4$. Ionization from the metal 3d orbitals of $Cu(NO_3)_2$, having the occupancy $(b_1)^2(b_2)^2(a_1)^2(e)^3$, leads to a number of ionic states: ionization from the $(e)^3$ subshell yields $^3A_2$, $^1A_1$, $^1B_1$, or $^1B_2$ states and ionization from each of the doubly occupied b_1, b_2, or a_1 MOs results in a ^1E or ^3E ionic state. Intensity considerations show that not all the metal ionizations are contained under peak A; thus, in the He(II) spectra, the intensity ratio of the two regions corresponding to the ligand ionizations (A–E: F, G for $Ti(NO_3)_4$; B–G: H, I for $Cu(NO_3)_2$) is considerably greater for $Cu(NO_3)_2$ than $Ti(NO_3)_4$ (Table III), showing that ionizations other than those arising from the nitrates contribute to the peaks B–G in the spectrum of $Cu(NO_3)_2(g)$. A numerical comparison of the relative intensities of the bands in the PE spectra of $Ti(NO_3)_4(g)$ and $Cu(NO_3)_2(g)$ (Table III) indicates that the intensity contribution of the copper "d" ionizations in the region B–G, as compared to band A, is $(3.8 - 1.7)/0.2 \approx 10{:}1$, thus suggesting that the majority of the states arising from the "d" ionizations are contained in the region B–G. The location of the metal ionizations will be considered later with reference to the ionic states of $Cu(NO_3)_2$. By analogy with the assignment proposed for the PE spectrum of $Ti(NO_3)_4(g)$, the ionizations from the nitrate orbitals may be interpreted as follows: peaks C and D arise due to ionizations from the e, b_1, a_2, and e MOs that correlate with the $1a_2'$ and 1e″ MOs of NO_3^- (Table IV), peaks E, F, and G correspond to ionizations from the e, b_2, and a_1 MOs that correlate with the 4e′ MO of NO_3^- and give rise to the principal metal–nitrate bonding interactions, peak H contains ionizations from

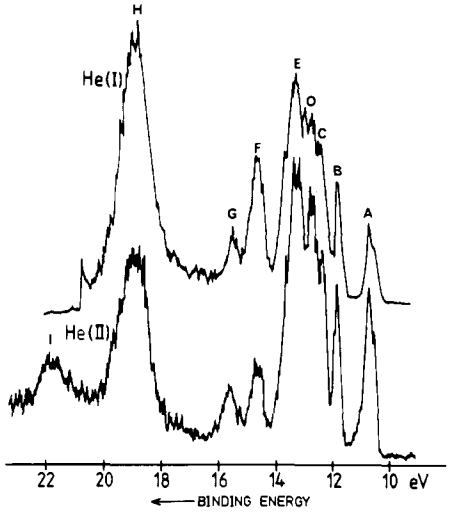

Figure 4. He(I) and He(II) photoelectron spectrum of $Co(NO_3)_3(g)$.

the a_1, b_2, e, and e MOs that correlate with the 3e′ and $1a_2''$ MOs of NO_3^-, and peak I contains the ionizations from the a_1 and b_2 MOs that correlate with the $4a_1'$ MO of NO_3^-. As in the case of $Ti(NO_3)_4$, the ionizations on the higher ionization energy side of the first main band, which correlate with the 4e′ MO of NO_3^- and are assigned to the metal-nitrate bonding orbitals, are more intense in He(I) than He(II). The shift of the IE for the feature which correlates with the 3e′ and $1a_2''$ N-O bonding orbitals, from 18.8 eV for $Ti(NO_3)_4(g)$ to 18.5 eV for $Cu(NO_3)_2(g)$, is consistent with the nitrato groups of the former having a slightly smaller effective negative charge than those of the latter. The ab initio calculation (vide infra) for $Cu(NO_3)_2$ estimates the formal overall charge on each nitrato group of $Cu(NO_3)_2$ to be −0.69 e (cf. −0.53 e for $Ti(NO_3)_4$[3]).

$Co(NO_3)_3$. The PE spectra of $Co(NO_3)_3(g)$ (Figure 4) are, as expected, similar to those of $Cu(NO_3)_2(g)$. The lowest energy ionization, A, absent in the spectra of $Ti(NO_3)_4(g)$ but present in the spectra of $Cu(NO_3)_2(g)$, clearly corresponds to ionizations from one or both of the cobalt 3d, e, and a_1 orbitals, expected from the cobalt(III), d^6 low-spin configuration[6] in D_3 symmetry.[11] The peaks B-E are assigned to ionizations from the a_2, e, a_1, a_2, e, and e MOs which correlate (Table IV) with the $1a_2'$ and 1e″ MOs of the nitrate groups. The higher energy region of E and the peaks F and G are assigned to the a_1, a_2, e, and e MOs which correlate with the 4e′ MOs of the nitrate groups. Again, the peaks to higher IE (for $Co(NO_3)_3(g)$, F and G) of the group that correlates with the 4e′ NO_3^- MOs have a greater relative intensity in He(I) than He(II) ionization, consistent with the general argument that these correspond to the metal-ligand bonding orbitals and contain some metal character. The broad band H in the spectrum of $Co(NO_3)_3(g)$ is assigned to ionizations from the a_1, a_2, e, e, a_2, and e MOs that correlate with the 3e′ and $1a_2''$ MOs of the nitrato groups. The highest IE peak in the He(II), (I), is assigned to the a_1 and e MOs that correlate with the $4a_1'$ MOs of the ligands. The intensity ratio of the region (B-G), compared with (H-I) in the He(II) spectrum for $Co(NO_3)_3(g)$ (Table III), is essentially the same as the corresponding value for $Ti(NO_3)_4(g)$, in contrast to $Cu(NO_3)_2(g)$, indicating that no metal ionizations are involved in the region (B-G) for $Co(NO_3)_3(g)$. Thus it is suggested that both the metal e and a_1 ionizations are contained under band A, the profile of which shows slight asymmetry in the sense expected for a_1 < e in IE. The IEs of the peaks H and I of $Co(NO_3)_3(g)$ are slightly higher than those of the corresponding features for $Ti(NO_3)_4(g)$ and thus the effective charge on each nitrato group of the former molecule would appear to be slightly less negative than that of the latter. This is consistent with the estimate of −0.46 e as the net charge per nitrato group of $Co(NO_3)_3$ by the ab initio calculation (vide infra).

Computational Details and Results

Ab Initio Calculation of $Cu(NO_3)_2$. Ab initio SCF calculations of the ^2E ground state of the D_{2d} configuration of $Cu(NO_3)_2$ were performed in a number of bases of Gaussian functions using geometrical parameters suggested by the electron-diffraction study of $Cu(NO_3)_2(g)$[11] and the structural details characterized for other nitrato complexes.[2] (Calculations on the other d^9 configurations of $Cu(NO_3)_2$ confirmed the ground state to be ^2E.) The first basis, denoted B1, is a basis of contracted Gaussian-type functions (GTFs) used to represent either Slater-type orbitals (STOs) or Hartree-Fock atomic orbitals. Best atom exponents[16] were used for all core orbitals, copper 4s, and nitrogen and oxygen 2s orbitals. For the copper 4p function an exponent of 1.2 was used. The metal 3d orbitals were represented by two STOs with exponents of 5.95 and 2.50.[17] All these orbitals were expanded in three GTFs/STOs. The nitrogen and oxygen 2p orbitals were Hartree-Fock atomic orbitals, each expanded in four GTFs.[18]

A more extensive basis set, denoted B2, employed a 12s, 6p, 4d Gaussian basis for Cu[19] and 7s, 3p basis for the ligand atoms.[20] These atomic sets are contracted to a 8s, 4p, 3d set for Cu and a 3s, 2p set for N and O.

Two extensions to B2 were considered.[21] First, this basis was incremented with a p function of exponent 0.32 in order to describe the Cu 4p atomic orbitals. This gives a 8s, 5p, 3d basis on Cu, denoted B2p. Second, an additional 3d function of exponent 0.20 was added, giving a 8s, 4p, 4d basis for Cu, denoted B2d.

Finally, a large basis set (14,9,5/9,5) contracted to (8,4,2/3,2) and denoted B3 is derived from the basis set of Wachters[22] for the copper atom and the basis set of Huzinaga for the nitrogen and oxygen atom.[23,24]

The valence MOs from the B1 basis are described in Table VI, together with the orbital and bond overlap populations. These results clearly point to $Cu(NO_3)_2$ providing a further example[25] of a complex in which Koopmans' theorem is not valid for those orbitals which are predominantly 3d in character. Thus, while the first experimental IE at 10.5 eV is undoubtedly due to a copper 3d electron, the corresponding calculated IEs lie beyond 19 eV, greater than both the N and O 2p ligand IEs. Results obtained with the other basis sets confirm that such a breakdown is not a function of the basis set.

Ligand IEs. These calculations provide a consistent interpretation of the MOs of $Cu(NO_3)_2$ which are concentrated primarily on the nitrato groups. The orbital energies from the small B1 basis set span the values predicted by B2 and B3; the greatest variation in a given ligand level with basis is ca. 1 eV and is generally much less than this. The predicted sequence of levels is independent of the basis and incrementing B2 with either diffuse p or d functions has little effect on the calculated ligand IEs. As presented below, a correlation of the $Cu(NO_3)_2$ ligand MOs (see Tables IV and VI) with those of the nitrate ion may be made, where the NO_3^- calculation performed in ref 3 used the same N and O basis orbitals employed in the present B1 study. This, together with the Koopmans' theorem IEs of Table VI, leads to an assignment of the peaks C-I of the PE spectrum of $Cu(NO_3)_2(g)$ (Figure 3) in agreement with that deduced by comparison with the PE spectrum of $Ti(NO_3)_4(g)$.

(i) The four highest filled orbitals of $Cu(NO_3)_2$, the 10e, $2b_1$, $1a_2$, and 9e, are closely spaced in energy (−14.4 to −15.1 eV) and correlate with the 1e″ (π) and $1a_2'$ (σ) oxygen lone pair

Table VI. Composition of the Valence Molecular Orbitals[a] of $Cu(NO_3)_2$

	atomic orbital character, %								
	Cu			N		O1, O2[b]		O3	
orbital[c]	d	s	p	s	p	s	p	s	p
7e (−20.6)	95						4		
$1b_1$ (−22.0)	99	1					1		
$9b_2$ (−22.0)	81			1	3			7	8
$10a_1$ (−23.4)	78	1			1	8	11		
10e (−14.4)			1		1		51		46
$2b_1$ (−14.6)	1						99		
$1a_2$ (−14.7)							100		
9e (−15.1)	1		1		3	3	61		31
8e (−15.6)	3		1				49		47
$11b_2$ (−16.5)	2		3		1		80	1	12
$12a_1$ (−17.2)		9	4			1	75	1	10
$11a_1$ (−21.3)	13				18	8	16	17	27
$10b_2$ (−21.5)	11				16	13	27	13	19
6e (−22.4)	1		2		27	16	34		19
5e (−23.1)					56		27		17
$8b_2$ (−25.4)	6		4	18		27	18	18	9
$9a_1$ (−25.4)	4	5		18		24	18	20	10
4e (−38.3)					24	72	2		
$7b_2$ (−40.9)			−1		33	29	4	33	2
$8a_1$ (−41.0)					33	28	4	32	3
$6b_2$ (−47.1)			−3	49		22	6	21	6
$7a_1$ (−47.0)				47		21	6	20	6

Atomic and Orbital Populations

	Cu			O1, O2		O3		N	
	s	p	d	s	p	s	p	s	p
population	6.3	12.3	9.1	3.8	4.6	3.8	4.3	3.3	3.3
formal charge		+1.38 e			−0.43 e		−0.18 e		+0.34 e

Cu-O Overlap Population[d]

Cu	O		Cu	O	
3d	2s	−0.002 (0.025)	4s	2p	0.054 (0.013)
3d	2p	−0.002 (0.126)	4p	2s	0.097 (0.064)
4s	2s	0.045 (0.028)	4p	2p	0.059 (0.013)
		total 0.251 (0.224)			

[a] B1 basis. [b] In all tables, O1, O2 are the oxygen atoms of the NO_3 group bonded to the metal atom, O3 being the terminal oxygen atom. [c] The corresponding orbital energy (eV) is given in parentheses. [d] Figures in parentheses refer to the Ti-O overlap population in $Ti(NO_3)_4$ (ref 3).

orbitals of the ligands. Ionizations from these MOs are correlated with the peaks in the spectral regions C and D.

(ii) The next three MOs, the 8e, $11b_2$, and $12a_1$, lying between −15.6 and −17.2 eV, correlate with the 4e′ nitrate orbitals which are mainly oxygen $2p_\sigma$ in character. All the calculations suggest, however, that the $12a_1$ MO has a significant copper 4s character (B1 estimate 9%) and provides a major contribution to the metal-oxygen (2p) overlap population. Ionizations from these MOs are considered to give rise to the peaks E, F, and G, respectively.

(iii) Three (the $11a_1$, $10b_2$, and 6e) of the four MOs lying between −21.3 and −23.1 eV correlate with the 3e′ (N-O σ bonding) MOs of the ligands and, of these, the $11a_1$ and $10b_2$ have a significant contribution from the metal 3d orbitals. The 5e orbital correlates with the N-O π-bonding ($1a_2''$) MOs of the nitrato groups. Peak H in the PE spectrum is attributed to ionizations from these four MOs.

(iv) The $8b_2$ and $9a_1$ MOs of $Cu(NO_3)_2$ at −25.4 eV correlate with the $4a_1'$ ligand orbitals. They involve 4% copper 4p and 5% copper 4s character (B1 estimates), respectively, and provide significant contributions to the metal-oxygen overlap populations. Ionizations from these two MOs are considered to be responsible for peak I.

The remaining MOs of $Cu(NO_3)_2$ associated primarily with the ligands are considerably more tightly bound; of these, the (4e, $7b_2$, and $8a_1$) and the ($6b_2$ and $7a_1$) correlate with the 2e′ and $3a_1'$ orbitals, respectively, of the nitrato groups.

Nature of the Metal–Ligand Interaction. A comparison of the components of the metal-oxygen overlap populations (Table VI) calculated for $Ti(NO_3)_4$ and $Cu(NO_3)_2$ suggest that the major bonding interaction in the titanium complex, that involving the metal 3d and oxygen 2p, is significantly reduced in $Cu(NO_3)_2$. The dependence of the overlap populations on basis set which is found may be rationalized in terms of the number and type of metal basis functions present. All the basis sets contain s functions of appropriate exponent to describe bonding through the 4s orbitals of copper. Indeed, the Cu 4s interaction with the oxygen 2s and 2p orbitals is found to provide a significant contribution to metal-ligand bonding in all calculations, with the 4s population varying from 0.28 e (B1) to 0.37 e (B2d). The 4s interaction is predicted to be the only bonding term in the B2, B2d, and B3 calculations; none of these basis sets contains functions of appropriate exponent to describe the copper 4p orbital. When such functions are included (B2p, B1) we find a significant Cu 4p interaction with the coordinated oxygen 2s and 2p orbitals, with the Cu 4p population varying from 0.23 e (B2p) to 0.29 e (B1).

The net charge calculated for the Cu atom varies with basis set according to the above considerations. Those basis sets with both s and p diffuse Cu functions lead to a formal charge of approximately +1.4 e, which is increased to +1.6 e (B2, B3) on removing the 4p function. The net loss of electron density per nitrato group decreases accordingly from ca. 0.30 e to ca. 0.19 e on removing the metal 4p functions. Even this former

Table VII. Assignment of the PE Spectrum of $Cu(NO_3)_2(g)$ by CI and Xα Methods

CI calculation			exptl		Xα calculation	
dominant configuration	states of $Cu(NO_3)_2$	calcd IE, eV	IE, eV	assignment	calcd IE, eV	orbital
$(7e)^2$	$^3A_2$	12.7	10.47(4)	(A)	12.2	10e
	$^1B_1, ^1B_2, ^1A_1$	12.9-13.4				
$(10a_1)^1, (9b_2)^1, (1b_1)^1$	$^{3,1}E$	13.7-14.6	11.65(4)	(B)	13.4	9e
					13.4	$2b_1$
$(2b_1)^1, (1a_2)^1$			12.17(3)	(C)	13.6	8e
$(10e)^3$	$^3A_1, ^1A_2, ^3B_2, ^3B_1$	14.2-14.3			13.9	$1a_2$
$(9e)^3$	$^{3,1}(A_1,A_2,B_1,B_2)$	14.7-15.1	12.63(4)-13.06(5)	(D)	14.4	$12a_1$
					14.4	$11b_2$
					15.7	$1b_1$
$(8e)^3$	$^{3,1}(A_1,A_2,B_1,B_2)$	16.6-17.0	13.68(3)	(E)	15.8	$10b_2$
$(11b_2)^1$	$^{3,1}E$	16.3-16.4	14.20(4)	(F)	15.9	7e
$(12a_1)^1$	$^{3,1}E$	16.9-17.2	15.35(4)	(G)	16.7	$11a_1$

value is considerably less than that in $Ti(NO_3)_4$, where a B1-type basis gave a loss of electron density of ca. 0.5 e per nitrato group.[3] The calculated atomic charges in both complexes (see Table VI, and Table III of ref 3) suggest that this loss of density involves chiefly the terminal oxygen atom (O3): the electron density of the nitrogen atom and the oxygen atoms coordinated to the metal (O1, O2) remain close to that found in the free nitrate anion.[3] Thus coordination results in a net drift of charge across the nitrato group, from the terminal oxygen to the metal atom. This drift is also reflected in the calculated oxygen 1s ionization potentials. The core ionization potential for the terminal oxygen atoms in $Cu(NO_3)_2$ is calculated to be 3.7 eV (B1 estimate) greater than the value for the coordinated oxygen atoms, in line with the calculated charge distributions. This shift in core ionization potential is slightly greater than the value of 3.4 eV predicted in the titanium complex.[3]

Based on the above analysis, it is tempting to suggest that the nature of metal-ligand bonding is quite different in $Ti(NO_3)_4$ and $Cu(NO_3)_2$, with the predominant interactions in the former involving the metal 3d orbitals while those in the latter involve the metal 4s and 4p orbitals. However, such a conclusion must be considered tentative in the light of the questionable significance of a Mulliken analysis in the framework of basis sets involving diffuse functions. Indeed, the significant 4s and 4p populations found in calculations on $[CuCl_4]^{2-}$ [26] have been attributed to the role of these functions in improving the chlorine 3s orbitals, rather than to their involvement in Cu-Cl bonding. Although it is difficult to quantify this ligand improvement effect, it is not unreasonable to assume that the use of a double ζ representation of the ligand valence orbitals in the present study (B2 and B3) would reduce the effect relative to that of ref 26, where a minimal basis set was used for the Cl 3s functions. Thus, the prediction of a significant involvement of the metal 4s and 4p functions in the copper-nitrate bonding interactions may not be entirely erroneous.

Configuration Interaction Calculation of the IEs of $Cu(NO_3)_2$. In view of the failure of Koopmans' theorem to provide a realistic picture of ionization from the Cu 3d orbitals, we first attempted to calculate such IEs by the ΔSCF method. From such a calculation, the ground state of $Cu(NO_3)_2^+$ was predicted to be the $^3A_2$ state corresponding to ionization from the 7e MO. However, it was found to be impossible to converge on many of the individual ionic states, arising from ionization of the other occupied metal and ligand MOs, due to the large degree of orbital relaxation accompanying metal electron ionization. Therefore, we have investigated the calculation of the valence IEs by a configuration interaction (CI) treatment designed to include relaxation effects, particularly those associated with ionization from the metal orbitals. The reference set used composed all of the configurations arising from a single valence electron ionization from the ground state of $Cu(NO_3)_2$ (Table VI). The orbitals obtained from an SCF calculation (B1 basis) on the $^3A_2$ state of the positive ion characterized by the metal orbital occupancies . . . $(10a_1)^2(9b_2)^2(1b_1)^2(7e)^2$ were used to construct these configurations. With the core orbitals remaining doubly occupied, all internal excitations relative to this configuration reference set were generated, the calculations being performed in effective C_{2v} symmetry.

While this truncation of the orbital space will clearly inhibit recovery of the orbital relaxation associated with ionization from ligand orbitals, particularly since the orbital set employed is that relevant to ionization of a Cu 3d electron, it is felt that the procedure should allow for a meaningful treatment of relaxation accompanying ionization from the copper 3d orbitals. An advantage of such a CI calculation, over a conventional ΔSCF approach, is that all the ionic states thus calculated will be orthogonal. A summary of the spectrum thus calculated is given in Table VII, together with the experimental features.

Considerable orbital relaxation is indeed predicted when ionization occurs from an orbital exhibiting a large metal d component. Thus the first band in the spectra is now attributed to ionization from the partially filled metal 7e orbital. The $^3A_2$ state, with an IE of 12.7 eV, is predicted to be the ground state of $[Cu(NO_3)_2]^+$, while the corresponding singlet states of A_1, B_2, and B_1 symmetry are calculated to lie between 12.9 and 13.4 eV. We thus predict that peak A in the PE spectra of $Cu(NO_3)_2(g)$ (Figure 3) arises from the ionization of the $(e)^3$ metal d electrons. The substantial relaxation associated with the ionization from the closed-shell metal orbitals ($10a_1$, $9b_2$, $1b_1$) places the associated $^{1,3}E$ states very close in energy to those states of the $[Cu(NO_3)_2]^+$ ion derived from ligand ionization from the $2b_1$, $1a_2$, and 10e ligand orbitals; all of these states are predicted to lie between 13.7 and 14.6 eV and are correlated with peaks B and C in the PE spectrum. A more definitive assignment of contributors to the individual peaks B and C is not possible from this calculation. The CI calculation does not change the assignment of the peaks D, E, F, and G from that given by Koopmans' theorem.

SW-Xα Calculation of IEs of $Cu(NO_3)_2$. A SW-Xα calculation of the ground state of $Cu(NO_3)_2$ was carried out using "muffin-tin" potentials together with calculations of the valence IEs using the transition-state method.[27] The calculations were performed using the spin-restricted approximation.[28] The atomic exchange parameters (α_{HF}) were those obtained by Schwarz.[29] For the extramolecular and intersphere regions, a weighted average of the atomic exchange parameters was used, the weights being the number of valence electrons in the neutral atoms. The outer sphere was placed externally tan-

Table VIII. Ionization Energies and Population Analyses of $Cu(NO_3)_2$ Calculated by the SW-Xα Method

orbital	calcd IE, eV	orbital population analyses, %							
		$\overline{Q}^n$(Cu)	$\overline{Q}^n$(N)	$\overline{Q}^n$(O3)	$\overline{Q}^n$(O1, O2)	QL^n(Cu)	QL^n(N)	QL^n(O3)	QL^n(O1, O2)
10e	12.2	51.5	0.3	6.0	42.1	23.1	2.8	32.8	41.3
9e	13.4	2.5	0.3	86.3	10.9	10.0	4.6	51.9	33.5
$2b_1$	13.4	46.8	0.0	0.0	53.2	18.6	1.9	29.8	49.8
8e	13.6	1.5	0.7	46.5	51.3	11.2	3.3	38.9	46.6
$1a_2$	13.9	0.0	0.0	0.0	100.0	9.8	1.2	25.0	64.0
$12a_1$	14.4	91.0	0.2	0.0	8.7	41.4	2.8	35.5	20.4
$11b_2$	14.4	86.4	0.3	0.6	12.7	33.8	2.8	35.1	28.3
$1b_1$	15.7	60.4	0.0	0.0	39.6	45.3	3.2	38.4	13.0
7e	15.9	51.5	1.5	2.5	44.6	31.4	3.1	34.3	31.2
$10b_2$	15.8	25.7	0.4	2.5	71.5	19.8	1.6	29.2	49.2
$11a_1$	16.7	30.6	1.0	3.3	65.1				
6e	19.0	1.1	45.9	21.9	31.0				
5e	22.0	3.9	23.8	4.6	67.7				
$9b_2$	22.0	0.2	16.5	58.7	24.6				
$10a_1$	22.0	0.3	16.4	58.5	24.9				
$8b_2$	23.6	1.6	15.2	26.0	57.2				
$9a_1$	23.6	2.0	15.5	26.0	56.5				

gential to the outermost atomic sphere. The calculations were carried out using overlapping atomic spheres with radii determined by the method of Norman[30] giving radii for the Cu, N, O3, and O1 spheres of 1.2457, 0.8055, 0.8940, and 0.9203 Å, respectively. Spherical harmonics up to $l = 3, 2, 1, 1$, and 1 were used to expand the outer, Cu, N, O3, and O1 regions, respectively. After convergence, the number of electrons within the Cu, N, O3, O1, intersphere, and outer-sphere regions were 28.24, 5.95, 7.78, 7.82, 3.98, and 0.06, respectively. To examine the charge migration occurring upon ionization, we have carried out a population analysis of the SW-Xα orbitals resulting from the ground-state and transition-state calculations. The quantities $\overline{Q}^n$(A) and QL^n(A) previously defined[31] give, respectively, for orbital n the gross population associated with the group of symmetry equivalent atoms A, and the corresponding charge loss occurring at the atoms A accompanying ionization from orbital n. These values are shown in Table VIII, together with the calculated IEs, the assignment of the PE spectrum being summarized in Table VII. The ground state of $Cu(NO_3)_2$ is predicted to be ^2E with the unpaired electron occupying an orbital having 51% Cu character compared to 95% in the ab initio calculation. Although there are a_1 and b_2 orbitals having close to 90% Cu character, the b_1 "metal" orbital has only 47% Cu character. There are thus two e (7e, 10e), and two b_1 ($1b_1$ and $2b_1$) orbitals having appreciable metal character.

The calculated IEs (Table VII) provide an interpretation of the PE spectrum of $Cu(NO_3)_2$ (Figure 3) that is in good overall agreement with that given by the ab initio CI calculation (vide infra):

(o) The lowest IE (A) is predicted to arise from the partially occupied 10e MO with considerable copper character, the calculated IE (12.2 eV) being close to that obtained from the CI calculation (12.7 eV).

(i) As obtained from the CI calculation, the Xα calculation predicts a group of ionizations, separated from the first IE by ca. 1 eV and which span an energy range of ca. 1 eV. This group includes the IEs from the highest filled b_1 orbital having substantial metal character, the mainly metal $12a_1$ and $11b_2$ orbitals, and the 8e, 9e, and $1a_2$ orbitals that correlate with the $1a_2'$ and 1e″ orbitals of the nitrato groups. These ionizations are considered to be manifest as peaks B, C, and D in the PE spectrum. As discussed with respect to the ab initio results, a definitive assignment of the peaks B and C is not possible with (Table VII) IEs of predominantly copper orbitals overlapping with those of mainly nitrate character. However, the CI and the Xα results suggest different assignments for peak D; the former attributes this to ionization from the mainly ligand based 9e MO, whereas the latter suggests that it corresponds to the IEs of the predominantly metal $12a_1$ and $11b_2$ MOs. Furthermore, the Xα calculation does not include the $1b_1$ MO which correlates with the nitrate 1e″ orbitals within the spectral region B-D, as suggested by the ab initio calculations. Given the clear correlation of the PE spectra from NO_3^- to $Ti(NO_3)_4$(g) and $Cu(NO_3)_2$(g), we favor the conclusions arrived at by the ab initio rather than the Xα calculations in these latter two respects.

(ii) There is then calculated to be a gap of 1.3 eV before ionization from the $1b_1$ and the 7e and $10b_2$ MOs which correlate with the 1e″ and 4e′ orbitals, respectively, of the nitrato groups; ionization from the $11a_1$ MO, which also correlates with the 4e′ nitrate orbitals, is calculated to occur ca. 1 eV to higher energy. Thus, apart from the involvement of the $1b_1$ MO, the results are in broad agreement with those obtained from the ab initio procedures, with the PE spectral features E and F arising from $1b_1$, 7e, and $10b_2$ ionization and G arising from $11a_1$ ionization.

(iii) and (iv) The results obtained from the Xα calculation agree with the ab initio assignment of bands H and I in the PE spectrum of $Cu(NO_3)_2$(g). Peak H is attributed to ionizations from the 6e, 5e, $9b_2$, and $10a_1$ MOs and peak I to ionization from the $8b_2$ and $9a_1$ MOs. The former group correlates with the 3e′ and $1a_2''$ and the latter group correlates with the $4a_1'$ orbitals of the ligands.

Ab Initio and SW-Xα Calculation on $Co(NO_3)_3$. An ab initio SCF calculation of the $^1A_1$ ground state of $Co(NO_3)_3$, using the geometrical parameters characterized[9] for $Co(NO_3)_3$(c), was carried out in a Gaussian basis analogous to B1 used for $Cu(NO_3)_2$, the results being shown in Table IX. As in $Cu(NO_3)_2$, the highest filled orbitals are localized on the ligands, the metal orbitals (e, a_1) occurring to considerably lower energy. In view of the larger basis size, it was not possible to carry out a CI calculation similar to that performed for $Cu(NO_3)_2$. However, in order to estimate the relative positions of ligand and metal ionizations, SCF calculations were carried out on the ionic states arising from ionization of the highest filled ligand orbital ($^2A_2$) and the e and a_1 metal orbitals (^2E, $^2A_1$), leading to calculated IEs of 15.0, 16.0, and 15.7 eV, respectively. These results are in disagreement with the experimental conclusion that the first peak in the PE spectrum corresponds to metal ionization, but are in agreement with the experimental suggestion that both metal ionizations contribute to a single peak in the spectrum. The assignment of peak A to the two metal ionizations allows the remaining bands in the spectrum to be assigned using Koopmans' theorem and the computational results of Table IX. Peaks B and C are assigned

Table IX. Calculations of Electronic Structure of $Co(NO_3)_3$ and the Assignment of the PE Spectrum of $Co(NO_3)_3(g)$

	atomic orbital character, %[a]									energy, eV		
	Co			N		O1, O2		O3				exptl
orbital	d	s	p	s	p	s	p	s	p	ab initio	SW-Xα	IE
$10a_1$	81					2	8	4	3	−24.7 (15.7)[b]	14.2	10.79(3) (A)
11e	58			2	16		15	4	6	−25.6 (16.0)[b]	13.5	
$9a_2$							54		45	−15.1 (15.0)[b]	13.7	11.89(3) (B)
19e	1						53		44	−15.3	13.7	12.42(11) (C)
$8a_2$			1			3	91		4	−15.9	14.2	12.85(15) (D)
18e							96		2	−16.1	14.6	
17e					2	3	56		38	−16.4	15.3	
$13a_1$	2						98			−16.4	15.7	13.28(4) (E)
$7a_2$			2		1		19		77	−16.7	15.1	
16e	3		1			1	52		41	−16.9	16.1	
15e	14		1		2	3	65		14	−18.3	17.5	14.66(4) (F)
$12a_1$	1	5				3	75	2	13	−19.0	17.6	15.57(7) (G)
$11a_1$	15				16	8	19	16	24	−22.5		
14e	14				18	8	19	16	24	−22.5		
$6a_2$			3		32	14	32		19	−23.6		
13e	15				36	7	25	1	15	−23.8		18.95(10) (H)
12e	14				30	9	30	1	14	−24.1		
$5a_2$					52	2	30		15	−24.4		

formal atomic charges: Co +1.5 e; N +0.37 e; O1, O2 −0.33 e; O3 −0.17 e

[a] Ab initio results. [b] Value estimated from SCF calculation on the corresponding ionic state.

to the $9a_2$ and 19e MOs, respectively, that correlate with the $1a_2'$ MO of NO_3^-, peak D to the $8a_2$ and 18e MOs that correlate with the $1e''$ MO of NO_3^-, and the most intense peak E with the 17e, $13a_1$, $7a_2$, and 16e MOs that correlate with the $1e''$ and $4e'$ MOs of NO_3^-. It is noteworthy that in D_3 for $Co(NO_3)_3$ but not in D_{2d} for $Ti(NO_3)_4$ and $Cu(NO_3)_2$ there is a combination of the nitrato group a_2' orbitals (a_2) which can have no metal d character. Such a restriction may account for the observation that $Co(NO_3)_3(g)$, but not $Cu(NO_3)_2(g)$ or $Ti(NO_3)_4(g)$, has the first ligand peak completely resolved. The ab initio calculation nicely predicts the two peaks F and G that are well separated from the broad band (C-E) to be due to the 15e and $12a_1$ MOs that also correlate with the $4e'$ MO of NO_3^-; the first of these has significant cobalt 3d character and provides the largest contribution to the Co-O bond overlap population. Peaks H and I are calculated to be due to orbitals that correlate with the ($1a_2''$, $3e'$) and $4a_1'$ MOs of NO_3^-, respectively.

A SW-Xα calculation, similar to that used to calculate the IEs of $Cu(NO_3)_2$, was carried out on $Co(NO_3)_3$. The results of this calculation show a similar trend to those discussed in detail for $Cu(NO_3)_2$, so that we only report the calculated IEs, shown in Table IX. Here it should be noted that the a_1 and e orbitals, that correlate with the $10a_1$ and 11e MOs of the ab initio calculation, have similar metal character (78, 66%) to the ab initio MOs. In contrast to the ab initio calculation, the SW-Xα method predicts the first ionization to arise from the metal e orbital, with the first ligand and metal a_1 ionization being to 0.2 and 0.7 eV higher energy, respectively. This is in disagreement with the PE spectrum, where the separation of the first two bands is ~1 eV. However, as in the case for the ab initio method, the ligand region of the spectrum can be satisfactorily assigned on the basis of the transition-state IEs (Table IX), except that the separation between bands F and G, which we have assigned to 15e and $12a_1$ ionizations, is not well reproduced by the Xα calculation.

Conclusions

In the PE spectra of all four molecules there are three main regions that can be clearly correlated with the ($1a_2'$, $1e''$, $4e'$), ($1a_2''$, $3e'$), and $4a_1'$ MOs, respectively, of the nitrate ligands. In the PE spectra of the Ti, Cu, and Co complexes, there are well-resolved peaks to high IE of the first ligand band. These are assigned to orbitals which correlate with the $4e'$ orbitals of NO_3^-, and which are calculated to have rather more metal character than the ligand orbitals to lower IE. These orbitals also provide contributions to the metal-ligand bonding interaction. These peaks have a greater intensity in the He(I) than in the He(II) spectra, indicating that they are of a different character to the main ligand ionizations. However, the origin of such intensity changes is not fully understood since a general feature of increased excitation energy is usually to increase the relative intensity of metal ionization.[32] The ligand ionizations of these three complexes can be satisfactorily assigned by the use of Koopmans' theorem applied to the ab initio SCF MO wave functions. The use of the transition-state approximation within the SW-Xα method provides a similar interpretation of these regions of the spectra, although the two assignments differ in some details.

These ligand regions of the spectra also provide some information on the relative charge distributions in these four molecules. The vertical IE of the peak that correlates with the $3e'$ and $1a_2''$ MOs of NO_3^- (F in $Ti(NO_3)_4$, H in $Cu(NO_3)_2$, H in $Co(NO_3)_3$, and E in $VO(NO_3)_3$) is essentially the same in the Ti, V, and Co complexes (18.8 eV), but is some 0.3 eV smaller in $Cu(NO_3)_2$. This difference is reflected in the formal ligand charges calculated from the ab initio wave functions (−0.53 e for $Ti(NO_3)_4$, −0.46 e for $Co(NO_3)_3$, and −0.69 e for $Cu(NO_3)_2$), which presumably arises from the greater number of d orbitals into which L → M electron donation can occur, for the Ti(IV), V(V), and Co(III) complexes, as compared to the Cu(II) complex.

The assignment of the metal ionizations in the Cu and Co complexes is not completely resolved. However, it is clear from the experimental data, that the first peak in the PE spectrum of both complexes arises from metal ionizations. Intensity considerations suggest that, in $Cu(NO_3)_2$, metal ionizations also contribute to the region B-D but that the corresponding region in the $Co(NO_3)_3$ spectrum (B-E) consists only of ligand ionizations. Neither of the theoretical treatments successfully locates the exact positions of the metal ionizations, although both predict that, in the case of $Cu(NO_3)_2$, they give rise to the first peak in the spectrum and are contained within the low IE region of the first ligand band. For $Co(NO_3)_3$ the calculations are less satisfactory: the ab initio ΔSCF method predicts the first IE to arise from ionization of a ligand orbital, and the SW-Xα method predicts the IE of the metal e orbital to be much closer to two ligand IEs than is observed experimentally.

Thus, for the molecules studied here, no strong preference can be expressed between a near minimal basis ab initio and a SW-Xα calculation for the interpretation of PE spectral data. However, it should be noted that we found the latter to be computationally more time consuming than the former, partly owing to difficulties encountered in converging the transition-state calculation for ionization from closely spaced ligand levels of the same symmetry.

Acknowledgments. We thank the Royal Society and The Science Research Council for financial support.

References and Notes

(1) (a) Manchester University; (b) Daresbury Laboratory.
(2) C. C. Addison and N. Logan, *Adv. Inorg. Chem. Radiochem.*, **6**, 71 (1964); C. C. Addison and D. Sutton, *Prog. Inorg. Chem.*, **8**, 195 (1967); C. C. Addison, N. Logan, S. C. Wallwork, and C. D. Garner, *Q. Rev., Chem. Soc.*, **25**, 289 (1971), and references cited therein.
(3) C. D. Garner, I. H. Hillier, and M. F. Guest, *J. Chem. Soc., Dalton Trans.*, 1934 (1975).
(4) C. D. Garner and S. C. Wallwork, *J. Chem. Soc.*, 1496 (1966).
(5) M. Schmeisser, *Angew. Chem.*, **67**, 493 (1955).
(6) R. J. Fereday, N. Logan, and D. Sutton, *Chem. Commun.*, 271 (1968).
(7) C. C. Addison and B. J. Hathaway, *Proc. Chem. Soc., London*, 19 (1957).
(8) M. Considine, J. A. Connor, and I. H. Hillier, *Inorg. Chem.*, **16**, 1392 (1977).
(9) J. Hilton and S. C. Wallwork, *Chem. Commun.*, 871 (1968).
(10) C. C. Addison and B. J. Hathaway, *J. Chem. Soc.*, 3099 (1958).
(11) A. A. Ischenko, E. Z. Zasorin, V. P. Spiridonov, and A. A. Ivanov, *Koord. Khim.*, **2**, 1203 (1976).
(12) B. Beagley, C. D. Garner, and R. Mather, unpublished results.
(13) R. A. Bowling, R. E. Sherrod, J. E. Bloor, J. D. Allen, Jr., and G. K. Schweitzer, *Inorg. Chem.*, **17**, 3418 (1978).
(14) A. A. MacDowell, C. D. Garner, I. H. Hillier, C. Demain, J. C. Green, E. A. Seddon, and M. F. Guest, *J. Chem. Soc., Chem. Commun.*, 427 (1979).
(15) P. Burroughs, S. Evans, A. Hamnett, A. F. Orchard, and N. V. Richardson, *J. Chem. Soc., Faraday Trans. 2*, **70**, 1895 (1974).
(16) E. Clementi and D. L. Raimondi, *J. Chem. Phys.*, **38**, 2686 (1963).
(17) J. W. Richardson, W. C. Nieuwpoort, R. R. Powell, and W. F. Edgell, *J. Chem. Phys.*, **36**, 1057 (1962).
(18) R. F. Stewart, *J. Chem. Phys.*, **50**, 2485 (1969).
(19) B. Roos, A. Veillard, and G. Vinot, *Theor. Chim. Acta*, **20**, 1 (1971).
(20) B. Roos and P. Siegbahn, *Theor. Chim. Acta*, **17**, 209 (1970).
(21) J. Demuynck and A. Veillard, *Theor. Chim. Acta*, **28**, 241 (1973).
(22) A. J. H. Wachters, *J. Chem. Phys.*, **52**, 1033 (1970).
(23) S. Huzinaga, *J. Chem. Phys.*, **42**, 1293 (1965).
(24) T. H. Dunning, Jr., *J. Chem. Phys.*, **53**, 2823 (1970).
(25) M. F. Guest and I. H. Hillier, "Quantum Chemistry, the State of the Art", V. R. Saunders and J. Brown, Eds., Atlas Computing Laboratory, Chilton, Didcot, Oxfordshire, 1975, p 205.
(26) J. Demuynck, A. Veillard, and U. Wahlgren, *J. Am. Chem. Soc.*, **95**, 5563 (1973).
(27) J. C. Slater, "Quantum Theory of Molecules and Solids", Vol. 4, McGraw-Hill, New York, 1974.
(28) K. H. Johnson, *Adv. Quantum Chem.*, **7**, 143 (1973).
(29) K. Schwarz, *Phys. Rev. B*, **5**, 2466 (1972).
(30) J. G. Norman, Jr., *J. Chem. Phys.*, **61**, 4630 (1974).
(31) M. Doran, R. W. Hawksworth, and I. H. Hillier, *J. Chem. Soc., Faraday Trans. 2*, **76**, 164 (1980).
(32) D. E. Eastman and J. L. Freeouf, *Phys. Rev. Lett.*, **34**, 395 (1975).

Theoretical Studies on the Physical Properties and Bonding of the 5d Metal Hexafluorides Using the Multiple Scattering Xα Technique

J. E. Bloor* and R. E. Sherrod

Contribution from the Chemistry Department, University of Tennessee, Knoxville, Tennessee 37916. *Received September 24, 1979*

Abstract: Nonrelativistic overlapping spheres Xα multiple scattering OSMSXα calculations have been performed on the 5d heavy metal hexafluorides MF_6, where M = W, Re, Os, Ir, Pt, and Au, and on MoF_6 and SF_6. With the aid of these calculations a consistent interpretation of the ionization potentials (IPs), electron affinities (EAs), and charge transfer (CT) electronic absorption bands for these molecules is obtained. The calculations are also shown to be successful in interpreting molecular properties related to the charge-density distributions. The method is found to be very useful in predicting trends in all the properties across the 5d series. Relativistic effects are discussed, and for the EAs it is found necessary to take into account these effects. After a semiempirical correction factor of ~1.0 eV, deduced from the molecular spin-orbit coupling constants is applied, the EAs are found to agree well with the most recent experimental estimates.

Introduction

There has been in recent years considerable interest shown in the properties of the 5d hexafluorides.[1-9] Part of this interest stems from the extraordinarily high electron affinities (EAs) (3-10 eV) of these molecules.[4] There have been a number of attempts to measure these experimentally but only upper and lower bounds have been established.[1-4] Moreover, apart from the original empirical rationalizations of Bartlett,[4] there have been no attempts to account for the relatively large EAs, in terms of their bonding features, either through actual calculation or even qualitatively. The recent success of the multiple scattering Xα technique (MSXα)[10-12] in calculating the EAs of a number of different types of atoms[13] and molecules[14-17] indicates that this method may yield results of sufficiently high quality to account for the observed EAs. Also, there have been a number of theoretical calculations on the ionization potentials[18,19] (IPs) and ultraviolet transitions[5-9,18,19] of some of these 5d metal fluorides using different methods than the MSXα technique. There has also been a previous nonoverlapping spheres MSXα calculation on WF_6[20] and one on PtF_6.[21]

Thus this series of molecules seemed to be an ideal set with which to test out our proposed overlapping spheres multiple scattering (OSMXα) method[17] both in comparison with other calculational methods and with experiment. In addition, the availability of the wave functions for this whole series of molecules has enabled us to discuss other physical properties of these molecules in a more detailed fashion than was possible previously.

Method of Calculation

The MSXα method is a nonvariational, self-consistent, one-electron technique involving the use of the Slater exchange approximation and the multiple-scattering formalism and has been described in detail elsewhere.[10-12] In addition to the experimental geometry, there are two types of theoretical pa-

0002-7863/80/1502-4333$01.00/0